Models and Signal Processing for an Implanted Ethanol Bio-Sensor

Jae-Joon Han, *Member, IEEE*, Peter C. Doerschuk*, *Senior Member, IEEE*, Saul B. Gelfand, and Sean J. O'Connor

***Abstract*—The understanding of drinking patterns leading to alcoholism has been hindered by an inability to unobtrusively measure ethanol consumption over periods of weeks to months in the community environment. An implantable ethanol sensor is under development using microelectromechanical systems technology. For safety and user acceptability issues, the sensor will be implanted subcutaneously and, therefore, measure peripheral-tissue ethanol concentration. Determining ethanol consumption and kinetics in other compartments from the time course of peripheral-tissue ethanol concentration requires sophisticated signal processing based on detailed descriptions of the relevant physiology. A statistical signal processing system based on detailed models of the physiology and using extended Kalman filtering and dynamic programming tools is described which can estimate the time series of ethanol concentration in blood, liver, and peripheral tissue and the time series of ethanol consumption based on peripheral-tissue ethanol concentration measurements.**

***Index Terms*—Bio-sensor, dynamic programming, ethanol consumption model, ethanol PBPK model, ethanol pharmacokinetics model, extended Kalman smoothing.**

I. Introduction

NEARLY 8% of people who use ethanol will become addicted during the course of their life [1], [2], and a large research effort of diverse content focuses on the effects of ethanol at levels ranging from the biochemical to the cognitive and behavioral. Measuring drinking behavior in natural settings over long time intervals is, so far, an unsolved problem. Even if such a record of voluntary ad-lib ingestion existed, the problem of deducing the true course of the individual's brain exposure to alcohol is compounded by a full range of absorption, distribution, and elimination kinetics across people ingesting the same drink.

This paper describes part of a system that is intended to open a new window on ethanol use by enabling unobtrusive measurement of the time course of ethanol concentration over periods of weeks to months in the community environment. Signal processing is an important part of this system. The sensor, a microelectromechanical systems transducer with a digital-to-analog converter, memory, and wireless telemetry link, is located subcutaneously to address safety and user acceptability issues. Therefore, only one ethanol concentration, that of peripheral tissue, is actually measured. The first important signal processing task is to estimate the time courses of the other important ethanol concentrations and of the oral ethanol consumption from the combination of noisy measurements of the peripheral-tissue ethanol concentration and knowledge of physiology. In many applications, the estimates are not needed in real time and/or the data are not available in real time; batch processing is of interest and it is this type of estimation problem that we consider in this paper.

We employ a model-based approach to estimating ethanol concentrations and oral ethanol consumption from the noisy measurements of peripheral-tissue ethanol concentration. The ethanol consumption (EC) model is a statistical model of the subject's drinking. The physiology models, specifically the gastrointestinal absorption (Gut) model and the physiologically-based pharmacokinetic (PBPK) model, are the models of ethanol absorption, distribution and elimination describing a particular individual and scalable across species. The EC, Gut, and PBPK models together form a generative model for the time course of ethanol. The subcutaneous bio-sensor (sensor) model is the measurement model.

Based on the sensor output and the generative model, the signal processing occurs in three major steps. The first step is to estimate the time course of all the state variables in the generative model by approximately computing the time-varying conditional means of all state variables using an Kalman filter (EKF) [3, Eqs. 8.1.1 and 8.1.2, p. 194] based on an approximation to the EC model. In order to improve the estimates, the second stage is maximum likelihood trajectory estimation for the oral-consumption time series based on the exact EC model treating the estimates from EKF as the measured input. This second stage is computed by a dynamic programming (DP) algorithm. The resulting estimates are state variables and state-transition times in the EC model. The third stage takes the state-transition times estimated by DP and estimates consumption rates that are piecewise constant by least squares. The results of these three stages of processing are accurate and robust estimates of the time series of ethanol concentration in blood, liver, and peripheral tissue and the time series of ethanol consumption. These estimates are of interest in and of themselves and as inputs to pattern classification to determine the subject's style of drinking.

Three key difficulties have to be overcome. First, the PBPK model is nonlinear and the state variables in the PBPK model

Manuscript received March 7, 2006; revised May 28, 2007. This work was supported in part by the National Institutes of Health under N01AA23102 and P60 AA07611-16-17; in part by the NIAA R01 AA12555-05; and in part by the National Science Foundation CCR-0098156. *Asterisk indicates corresponding author.*

J.-J. Han and S. B. Gelfand are with the School of Electrical and Computer Engineering, Purdue University, West Lafayette, IN 47907 USA (e-mail: jhan@purdue.edu; dearjay@yahoo.com; gelfand@ecn.purdue.edu).

*P. C. Doerschuk is with the Department of Biomedical Engineering and the School of Electrical and Computer Engineering, Cornell University, 305 Phillips Hall, Ithaca, NY 14853-5401 USA (e-mail: pd83@cornell.edu).

S. J. O'Connor is with the Department of Psychiatry, Indiana University School of Medicine and the R. L. Roudebush VA Medical Center, Indianapolis, IN 46202 USA.

Color versions of one or more of the figures in this paper are available online at http://ieeexplore.ieee.org.

Digital Object Identifier 10.1109/TBME.2007.912652

are masses of ethanol in different compartments, so the state variables are constrained to be positive. Second, the Gut model, though linear, has a time constant on the order of 30 min to 1 h so the oral consumption input is severely low-pass filtered before it even excites the PBPK model. Third, statistical modeling of the source, i.e., the oral consumption, is very challenging because of the range of drinking style across people.

The remainder of this paper is organized as follows. In Section II, the generative model is described, followed by a description of the conditional mean estimator in Section III. Parameter identification methods are described in Section IV. The second and third stages of processing, the maximum likelihood trajectory estimator and the piecewise constant mark level estimator, respectively, are described in Section V and results on the complete system are described in Section VI. Finally, a discussion follows in Section VII.

The following notation is used. Prime denotes vector or matrix transpose. "Independent and identically distributed", "probability mass function," and "probability density function" are abbreviated by "i.i.d.," "pmf," and "pdf," respectively. The unit step function is denoted by $u(\cdot)$ and the unit ramp function is denoted by $r(t) = tu(t)$. I_l is the $l \times l$ identity matrix and $0_{l,m}$ is the $l \times m$ zero matrix.

II. Model

A. PBPK Model of Ethanol Distribution and Elimination

The PBPK model is an interconnection of three so-called "well stirred" compartments which represent the vasculature, liver, and all other tissues (the "periphery"). Each compartment is described by giving the mass of ethanol in the compartment and the mathematical model for a compartment is a first-order nonlinear differential equation which describes the time rate of change of the mass of ethanol in the compartment. When ethanol enters a compartment, perfusion coefficients approximate the reality that ethanol is not instantly spread uniformly throughout the compartment but there remains a single ethanol concentration for each compartment. This is what is meant by "well stirred." Elimination of ethanol occurs from the liver compartment via a single enzyme system which follows Michaelis–Menten (MM) kinetics [4].

Ethanol enters the system through two pathways. The simpler pathway is by venous infusion, which occurs only in a laboratory setting. In this case, the ethanol is added directly to the well-stirred vascular compartment. The more complicated pathway is by oral intake; the ethanol is transported through the proximal gut, absorbed in the small intestine, and enters the portal vein before entering the liver. The Gut model describes the transport and absorption processes while the PBPK model has the mass flux of ethanol into the portal vein as its input.

The PBPK model is presented in detail in [5] and the equations for the PBPK model are listed in Appendix I. What matters here are the input, state, and output variables which need to be connected to the other components of the complete model. The external inputs to the PBPK model are the mass flows, denoted by $M_{\mathrm{Gut}}(t)$ and $M_{\mathrm{Infuse}}(t)$ (units of [Mass]/[Time]), which are the mass flow of ethanol from the gut into the portal vein and from a venous infusion directly into the vascular compartment, respectively. The state variables in the PBPK model are the masses of ethanol in each compartment, denoted by $\mu_{\mathcal{X}}(t)$ (units of [Mass]) where $\mathcal{X}$ takes values $\mathcal{V}$ for the Vascular, $\mathcal{T}$ for the peripheral Tissue, and $\mathcal{L}$ for the liver parenchyma. In addition, there are volumes for each compartment, denoted by $V_{\mathcal{X}}$, and concentrations for each compartment, denoted by $C_{\mathcal{X}}(t) \doteq \mu_{\mathcal{X}}(t)/V_{\mathcal{X}}(t)$. For the purposes of this paper, the output of the PBPK model is the peripheral tissue ethanol concentration which is $C_{\mathcal{T}}(t) \doteq \mu_{\mathcal{T}}(t)/V_{\mathcal{T}}(t)$.

Define the state vector, denoted by $\mathbf{x}_{\mathrm{P}}(t)$, by $\mathbf{x}_{\mathrm{P}}(t) \doteq (\mu_{\mathcal{V}}(t), \mu_{\mathcal{L}}(t), \mu_{\mathcal{T}}(t))'$, the vector-valued function for computing the derivative of the state vector, denoted by $f_{\mathrm{P}}(\cdot)$, by $f_{\mathrm{P}}(\cdot) \doteq (f_{\mathcal{V}}(\cdot), f_{\mathcal{L}}(\cdot), f_{\mathcal{T}}(\cdot))'$ where the functions $f_{\mathcal{X}}(\cdot)$ are defined in [5] and implied by the equations of Appendix I, $g_{\mathrm{P}} = (1,0,0)'$, and $h_{\mathrm{P}} = (0,0,1/V_{\mathcal{T}})'$. Then the PBPK model is

$$\frac{\mathrm{d}\mathbf{x}_{\mathrm{P}}}{\mathrm{d}t}(t) = f_{\mathrm{P}}\left(\mathbf{x}_{\mathrm{P}}(t), M_{\mathrm{Gut}}(t)\right) + g_{\mathrm{P}} M_{\mathrm{Infuse}}(t) \tag{1}$$

$$C_{\mathcal{T}}(t) = h_{\mathrm{P}}' \mathbf{x}_{\mathrm{P}}(t) \tag{2}$$

with initial conditions on $\mathbf{x}_{\mathrm{P}}(t_0)$ such that every component is positive.

B. Gut Model

The Gut model describes the transport of ethanol from oral ingestion through absorption in the intestines to the portal vein. As is described in detail in [6], the experimental data is consistent with a linear time-invariant system with a critically-damped second-order impulse response. Let $M_{\mathrm{oral}}(t)$ (units of [Mass]/[Time]) denote the oral input mass flow and $M_{\mathrm{Gut}}(t)$, which was defined in Section II-A, denote the mass flow from the gut into the portal vein. Let the impulse response be denoted by $h_{\mathrm{Gut}}(t)$. Then $h_{\mathrm{Gut}}(t) = \beta^2 t \exp(-\beta t) u(t)$ where the β^2 factor implies that $\int_{-\infty}^{+\infty} h_{\mathrm{Gut}}(t)dt = 1$ so that ethanol is conserved. The value of $1/\beta$ is on the order of 30 min. Notice that if $M_{\mathrm{Oral}}(t) \geq 0$ for all t then $M_{\mathrm{Gut}}(t) \geq 0$ for all t.

A state-space realization of $h_{\mathrm{Gut}}(\cdot)$ requires a 2-D state vector, denoted by $\mathbf{x}_{\mathrm{G}}$, and is not unique. The realization we have used is

$$\begin{aligned} \frac{\mathrm{d}\mathbf{x}_{\mathrm{G}}}{\mathrm{d}t}(t) &= F_{\mathrm{G}} \mathbf{x}_{\mathrm{G}}(t) + g_{\mathrm{G}} M_{\mathrm{Oral}}(t) \\ M_{\mathrm{Gut}}(t) &= h_{\mathrm{G}}' \mathbf{x}_{\mathrm{G}}(t) \end{aligned} \tag{3}$$

where the 2×2 matrix F_{G} has components $F_{\mathrm{G}}^{1,1} = F_{\mathrm{G}}^{2,2} = -\beta$, $F_{\mathrm{G}}^{1,2} = 0$, and $F_{\mathrm{G}}^{2,1} = \beta$, $g_{\mathrm{G}} \doteq [\beta\ 0]'$, and $h_{\mathrm{G}} = [0\ 1]'$. If nonzero initial conditions on $x_{\mathrm{G}}(t_0)$ are used, then they must be appropriate in order to retain the result that if $M_{\mathrm{Oral}}(t) \geq 0$ for all t then $M_{\mathrm{G}}(t) \geq 0$ for all t.

C. Ethanol Consumption (EC) Model

One of the goals of the signal processing is to determine as much as possible about the consumption of ethanol. However, the consumption of ethanol is separated from the sensor by two systems, the Gut and the PBPK systems, and both the Gut and the PBPK systems are relatively low-pass in character, compared to the sample interval. Therefore, a detailed model for the time course of the consumption of ethanol is necessary.

The key aspect of ethanol consumption in our analysis is the presence of periods of drinking and periods of no drinking. This approximation seems appropriate in humans, who tend to drink in small increments or else to retain larger amounts in their stomachs before it is released steadily for absorption in the gut. Therefore, a two-state continuous-time Markov chain [7], [8] is defined where State 1 corresponds to "no drinking" and State 2 corresponds to "drinking". Each state has a variable called a mark which is the rate of drinking (mass of ethanol per unit time). All the values of the marks in State 1 are 0 since State 1 corresponds to "no drinking". The marks in State 2 are drawn randomly at each state transition from State 1 to State 2 and remain the same while the Markov chain is in State 2. The mark drawn at the kth state transition from State 1 to State 2 is denoted by m_k. The sequence of random marks is i.i.d. with pdf or pmf denoted by $p_m(\cdot)$.

The temporal dynamics of the Markov chain are defined by the probability mass function on the initial state of the Markov chain and by the rates for transitions from State 1 to State 2 and from State 2 to State 1 which are denoted by $\lambda_{1,2}$ and $\lambda_{2,1}$, respectively. The largest time constant of the Markov chain, which is the inverse of the smallest eigenvalue of the 2×2 matrix of transition rates and has value about 6 h, is much smaller than the interval of interest which is about four weeks. Therefore, to avoid unnecessary additional parameter estimation associated with the initial state of the Markov chain it is assumed that the initial state is the steady state. The rate functions are required to be nonnegative but are otherwise unconstrained.

Using constant rates, it was difficult to get Markov chain trajectories that reflected the diversity of human drinking. For instance, no drinking for a long time (more than a day) is intermixed with daily (within a day) drinking. Therefore, time variation of the rates was introduced and, since little is known, stochastic time variation was used making this a doubly stochastic model. In particular, each rate is modeled as a mean plus a first-order autoregressive (AR) process driven by a white Gaussian stochastic process with zero mean and constant power spectral density $\sigma^2_{1,2}$ or $\sigma^2_{2,1}$ for $\lambda_{1,2}$ or $\lambda_{2,1}$, respectively. For the transition from State 1 to State 2, the rate model is

$$\lambda_{1,2}(t) = \lambda^0_{1,2} + \epsilon_{1,2}(t) \tag{4}$$

$$\frac{\mathrm{d}\epsilon_{1,2}}{\mathrm{d}t}(t) = \alpha_{1,2}\epsilon_{1,2}(t) + w_{1,2}(t) \tag{5}$$

where $w_{1,2}(\cdot)$ is a white Gaussian stochastic process with mean zero and power spectral density $\sigma^2_{1,2}$. The model for the transition from State 2 to State 1 is the same but with "1,2" replaced by "2,1." Notice that these models do not guarantee that the rates will be nonnegative and that constraint will be added when the rates are used.

D. Sensor Model

The sensor comprises a transducer, digital to analog converter, short-range wireless telemetry link, antenna, and battery all packaged into a capsule suitable for subcutaneous implantation. The transducer employs piezoresistive microcantilevers coated on one side with an ethanol-sensitive plastic. Transduction occurs in the vapor phase protected from molecules larger than ethanol by a nanoporous silicon membrane. The transducer is under simultaneous development so its precise performance is uncertain. However, the bandwidth of the Gut and PBPK systems is quite narrow and the sensor is broad-band in comparison. Preliminary tests indicate that the sensor will have a noise standard deviation that is less than 5% of the peak value. In addition to the noise, we consider a time varying bias which is modeled as a first-order AR process (denoted by $b[n]$). The requirement to save a series of sensed values for later telemetry is implemented digitally; thus, we treat the sensor as a discrete-time device. In order to save battery power, the discrete-time sampling interval, denoted by T, is on the order of 1 min. Therefore, by (2), the sensor model is

$$\begin{aligned} y[n] &= h'_{\mathrm{P}}\mathbf{x}_{\mathrm{P}}(nT) + b[n] + v[n] \\ b[n+1] &= \alpha b[n] + w[n] \end{aligned} \tag{6}$$

where $v[\cdot]$ and $w[\cdot]$ are independent, $v[\cdot]$ is an i.i.d. white Gaussian noise with zero mean and known variance σ^2, and $w[\cdot]$ is an i.i.d. white Gaussian noise with zero mean and known variance σ^2_w. Alternatively, the sensor can be modeled using a constant coefficient of variation (CCV) model which is $y[n] = (1+v[n])h'_P x_P(nT) + b[n]$. Numerical results showing the robustness of processing based on the model of (6) when truth is the CCV model are described in Section VI.

III. Time-Varying Conditional Mean of the State Variables

Using the model described in Section II, the goal is to compute estimates of the time-varying oral intake of ethanol ($M_{\mathrm{Oral}}(t)$) and the time-varying mass of ethanol in each of the three PBPK compartments ($\mu_{\mathcal{V}}(t)$, $\mu_{\mathcal{L}}(t)$, and $\mu_{\mathcal{T}}(t)$). However, the complexity of the model makes it intractable to compute exact estimates for any standard estimation criteria such as maximum likelihood.

One approach, as sketched in Section I, is to focus on conditional mean estimators and approximate computation of such estimators using the EKF [9]–[12] [3, Eqs. 8.1.1 and 8.1.2, p. 194] techniques. EKF techniques are designed for discrete-time models in the form

$$x_{k+1} = f_k(x_k) + g_k(x_k)w_k \tag{7}$$

$$z_k = h_k(x_k) + v_k \tag{8}$$

where w_k and v_k are i.i.d. Gaussian sequences with zero mean and known covariance. Therefore, the model of Section II requires alteration in two aspects: it must be transformed to discrete time and the EC part, which is the input model, must be approximated by a Gaussian model. In order to improve performance, a smoothing approach based on EKF ideas is used rather than a filtering approach directly using EKF ideas.

A. Gaussian Equivalent EC Model

The EC model described in Section II-C plays the role of the process noise w_k in (7). Because $M_{\mathrm{Oral}}(t)$, the output of the EC model, is not a Gaussian sequence, the EC model is approximated by a Gaussian model, which we refer to as the equivalent Gaussian model, with the same first- and second-order statistics.

In Appendix II, the equivalent Gaussian model is derived for the case where the rates $\lambda_{1,2}(t)$ and $\lambda_{2,1}(t)$ are constant with respect to time. The same state-space realization is used when the rates vary with time, in particular, when the rates are themselves stochastic processes as in (4) and (5), because the variations in the rates are arranged to be at a much slower time scale than the transitions in the Markov chain. Therefore, this is a quasi-static approximation.

A second issue concerns positivity. This arises in two senses. First, the Gut and PBPK models are designed for the case where $M_{\mathrm{Oral}}(t) \geq 0$ for all t. The choice of positive mean value in the Gaussian equivalent model typically results in such positivity with high probability but no Gaussian equivalent model guarantees positivity at all times, and, therefore, one of the standard methods is used to ensure the positivity. Specifically, a unit ramp function (which is defined at the end of Section I) is introduced which sets negative values of $M_{\mathrm{Oral}}(t)$ to 0. Alternatively, an absolute value or a squaring can be used. Second, the rates $\lambda_{1,2}(t)$ and $\lambda_{2,1}(t)$ are Gaussian autoregressive stochastic processes and, therefore, can take negative values. Therefore, before the rates of transition from no drinking to drinking and vice versa are used in the formulas for the quasi-static Gaussian equivalent model, they are passed through ramp functions which could also be replaced by the alternative methods.

In summary, based on Appendix II, the Gaussian equivalent EC model (with output $\tilde{M}_{\mathrm{Oral}}(t)$) is (4) and (5) and

$$\frac{\mathrm{d}\mathbf{x}_{\mathrm{EC}}}{\mathrm{d}t}(t) = F_{\mathrm{EC}}\left(r\left(\lambda_{1,2}(t)\right), r\left(\lambda_{2,1}(t)\right)\right)\mathbf{x}_{\mathrm{EC}}(t) + g_{\mathrm{EC}}\left(r\left(\lambda_{1,2}(t)\right), r\left(\lambda_{2,1}(t)\right)\right) w_{\mathrm{EC}}(t) \quad (9)$$

$$\tilde{M}_{\mathrm{Oral}}(t) = r\left(h'_{\mathrm{EC}}\mathbf{x}_{\mathrm{EC}}(t)\right) + \frac{m_p \lambda_{1,2}(t)}{\left(\lambda_{1,2}(t) + \lambda_{2,1}(t)\right)} \quad (10)$$

where $w_{\mathrm{EC}}(\cdot)$ is a zero-mean white Gaussian process with power spectral density 1, $F_{\mathrm{EC}}(\lambda_{1,2}, \lambda_{2,1}) = \mathrm{diag}(-\lambda_{2,1}, -(\lambda_{1,2} + \lambda_{2,1}))$, $h_{\mathrm{EC}} = [1\ 1]'$, $g_{\mathrm{EC}}(\lambda_{1,2}, \lambda_{2,1}) = [A\ B]'$, $A = \sqrt{2\lambda_{2,1}/(\lambda_{1,2}(\lambda_{1,2}+\lambda_{2,1}))}[\sqrt{m_m^2\lambda_{2,1}^2 + \sigma_m^2(\lambda_{1,2}+\lambda_{2,1})^2} - \sqrt{(m_m^2+\sigma_m^2)\lambda_{2,1}^2}]$, $B = \sqrt{2\lambda_{1,2}\lambda_{2,1}(m_m^2+\sigma_m^2)/(\lambda_{1,2}+\lambda_{2,1})} - A$, and m_m and σ_m^2 are the mean and variance of the mark distribution $p_m(\cdot)$. Notice that the Gaussian equivalent EC model depends only on the mean and variance of the mark distribution so more details of the mark distribution are not required.

B. Transformation to Discrete Time

The forward Euler approximation [13] is used to discretize the differential equations. The sampling intervals are T_h [PBPK, (1), Gut, (3) and Gaussian equivalent EC model, (9)] and T_λ [autoregressive models for the rates of the Markov chain transitions, (5)]. Consistent with the quasistatic approximation in Section III-A, we assure that $l = T_\lambda/T_h$ is an integer.

C. Fixed Lag Smoothing at Multiple Sampling Rates

Since, as described in Section I, this paper concerns batch processing, it is possible to compute the conditional mean of the state at time n given either all the measurements (a so-called fixed interval smoother) or the measurements up to and including time $n + L$ (a so-called L-order fixed lag smoother). In all batch processing cases with optimal estimators and no model mismatch, fixed interval smoothing has better performance than fixed lag smoothing. However, in a previous study of smoothing for finite-state Markov processes (the EC model belongs to this class), it was reported that beyond a certain lag there is no further improvement by increasing the number of lags [14]. That is, fixed lag smoothing with enough lags performs almost as well as fixed interval smoothing. For this reason, we use fixed lag smoothing with a large lag as seems typical in practice. In discrete time, a fixed lag smoother and a filter are closely related by state augmentation [3].

If the original state has dimension p and an L-order fixed lag smoother is desired then the augmented state (of dimension $(L+1)p$) contains the original state at the current time and each of the immediate past L times. The state update equation [3, Eq. 7.3.3, p. 177] has L block rows that are shifts and one block row that executes the original state update present in the original dynamical system.

In addition to different sampling rates for the discrete-time approximations to the PBPK, Gut, and Gaussian equivalent EC models (interval T_h) and the rates of the Markov chain transitions (interval T_λ), as described in Section III-B, it is natural to have different orders of lag. In particular, since the rates of the Markov chain transitions vary slowly, it is natural to have a much larger order lag for the rates than for the other variables. In particular, we have used lags of $L = 60$ min for the PBPK, Gut, and Gaussian equivalent EC variables and lags of $L = 24 \times 60$ min for the rates of the Markov chain transitions. For differences in lag order of this size, direct application of the augmentation idea of the previous paragraph leads to a high computational burden. However [15], it is possible to organize the computations so that the burden is reduced by a factor of 60.

As is described in Section VI-A, simulations were performed in order to determine an acceptable value for the lag L. Performance of the EKF was measured by the square root of the normalized mean square error defined in (11). Based on these results L is set to 60 min in the remainder of this paper.

IV. Identification of the Parameters

The single parameter of the Gut model, the time constant $1/\beta$ in Section II-B, and the parameters of the PBPK model are determined as described in [5], [6], [16], and [17]. The resulting values are[1] $1/\beta = 30$ min, $R_A = 50.3547$ dL/min, $V_{\mathcal{T}} = 23.5734$ L, $V_{\mathcal{V}} = 12.4899$ L, $V_{\mathcal{L}} = 1.7198$ L, $M_{\max} = V_{\mathcal{L}} V_{\max} = 134.47$ mg/min, and $k_{x,y} = 0.3243$ (for all values of x, y), $F_{\mathrm{L}} = .26$, $F_{\mathrm{PV}} = .75$, and $K_m = 10$ mg/dL where R_A, $V_{\max}$, $k_{x,y}$, K_m, F_{L}, and F_{PV} are defined in Appendix I.

For the sensor, the noise standard deviation σ is determined by qualitative examination of *in vitro* experiments with prototypes of the transducer, and has the value 5% of the maximum value of the peripheral tissue ethanol concentration, which is approximately two thirds of the common legal limit of 0.08 mg/dL. The parameters for the time varying bias are $\alpha = 0.7$ and $\sigma_w = 0.001/T_\lambda$.

[1] In keeping with the bulk of ethanol pharmacokinetic research, we use units of minutes (min) for time, liters (L) or deciliters (dL) for volume, centimeters (cm) for distance, and milligrams (mg) or kilograms (kg) for mass.

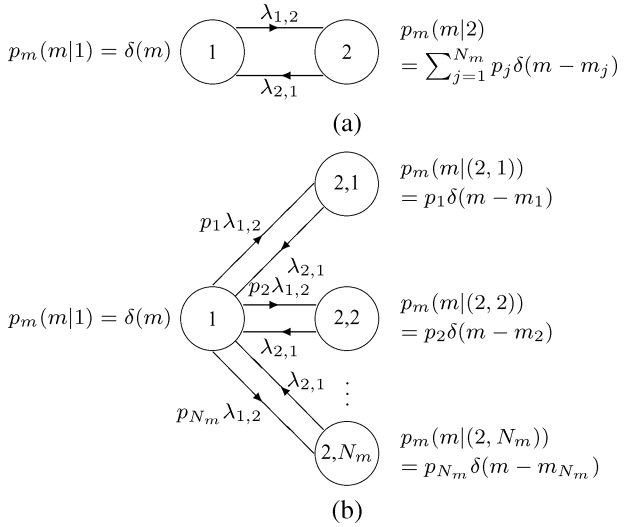

Fig. 1. EC: (a) finite number of mark levels possible in State 2; (b) one mark level possible in each of the states derived from State 2.

Continuous monitoring of interstitial fluid ethanol consumption has yet to be achieved in people; there are no *in vivo* ethanol consumption trajectories from which to estimate the parameters in the EC or Gaussian equivalent EC model. However, based on his clinical expertise, O'Connor has provided nine trajectories each of duration 4 weeks for nine different classes of ethanol user. The nine users are social drinker, binge drinker, salesman, two different graduate students, street person, working alcoholic, wine at dinner, and lunch and dinner drinker. Because the time series are of long duration, they are displayed as images in this paper (e.g., Fig. 4). Subsequently, these trajectories will be referred to as prototypical clinical oral ethanol input trajectories.

The six parameters describing the dynamics (three for the State 1 to 2 transition and three for the State 2 to 1 transition) were set based on qualitative ideas, e.g., $\lambda^0_{1,2}$ and $\lambda^0_{2,1}$ were set to the expected durations of an interval of drinking The resulting values are $\lambda^0_{1,2} = 0.0022(1/\text{min})$, $\lambda^0_{2,1} = 0.0167(1/\text{min})$, $\alpha_{1,2} = \alpha_{2,1} = -0.3/T_\lambda$, and $\sigma_{1,2} = \sigma_{2,1} = 0.001/T_\lambda$. The sampling intervals are $T_h = 1$ min (forward Euler discretization) and $T_\lambda = 60$ min (autoregressive Markov chain transition rate model).

The final parameter is the pdf or pmf on the marks conditional on being in the drinking state (State 2). Unlike the other parameters, this distribution is identified for each individual trajectory. First the range of human drinking rate is discretized into six levels. Then each level is assumed to have an equal prior probability. Finally, by approximately computing the likelihood for each discrete-level value by an EKF, the posterior pmf over the levels is computed. This pmf is then used in all of the signal processing.

V. Maximum Likelihood Trajectory Estimate of the Ethanol Consumption and Least Squares Estimation of Mark Levels

The EC model (Section II-C, Fig. 1) is a two-state continuous-time marked Markov chain. For computation, it is discretized with sampling interval $T_h = 1$ min which was chosen because the Gut model has a repeated pole with time constant 30 min. The goal is to compute the maximum likelihood state trajectory from measurements of the marks where the measurements are not perfect, i.e., if x_n (y_n) is the state (measurement) at time n and x_n^m (y_n^m) is the state trajectory (measurement trajectory) from time n to time m then the state trajectory estimate (itself a function of y_n^m) is $\hat{x}_n^m(y_n^m) = \arg\max_{x_n^m} \ln p(x_n^m|y_n^m)$. The corrupted measurements of the marks and the variances of the measurements are actually the oral input estimates from the EKF and the variances of the oral input estimates as calculated by the EKF. The EKF-computed variances are only an approximation to the true variances of the errors. The errors are correlated but the correlations are ignored in the derivation of the maximum likelihood trajectory estimator. To include the correlations would require additional modeling and parameter estimation, along with a significantly more complex maximum likelihood trajectory estimator implementation, which was not pursued here. However, the correlation between errors and states is included. The mean and variance conditional on the estimated states can be computed from the EKF-computed mean and variance and then applied to the maximum likelihood trajectory estimation. Significantly, this does not require any additional modeling.

For arbitrary probability distributions for the mark conditioned on the state, maximum likelihood trajectory estimation is very difficult, though perhaps it can be approximated by the types of methods described in [18]. However, if the probability distribution is discrete with a finite number of values, then the calculation is tractable, because the original Markov chain, shown in Fig. 1(a), is equivalent to a second Markov chain, shown in Fig. 1(b), which has only one possible mark value for each state. Then, with only one possible mark value for each state, the maximum likelihood trajectory estimation problem is a standard problem in hidden Markov models [19], which can be solved by forward dynamic programming.

The third and final stage of the processing is least squares estimation of mark levels using the Markov chain transition times that were determined in the second stage by DP and the continuous-valued oral input estimate determined in the first stage by the EKF. The time between an estimated State 1 (no drinking) to State 2 (drinking) transition and the following estimated State 2 to State 1 transition is divided into 60 min segments starting at the time of the estimated State 1 to State 2 trajectory and ending with a short segment just before the estimated State 2 to State 1 transition. Within each segment the estimated mark level is determined by solving a linear least squares problem where the regressor is a constant within the segment.

VI. Numerical Results

To evaluate the performance of the estimator in each stage, three quantitative criteria are considered. The first criterion is the square root of the normalized mean square error (MSE), which tracks sample-by-sample accuracy, and is defined by

$$\text{MSE} = \sqrt{\int \left| M_{\text{Oral}}(t) - \hat{M}_{\text{Oral}}(t) \right|^2 \Big/ \int |M_{\text{Oral}}(t)|^2}. \quad (11)$$

For ethanol research, it is important to accurately estimate the total amount of ethanol consumed and it would be desirable for

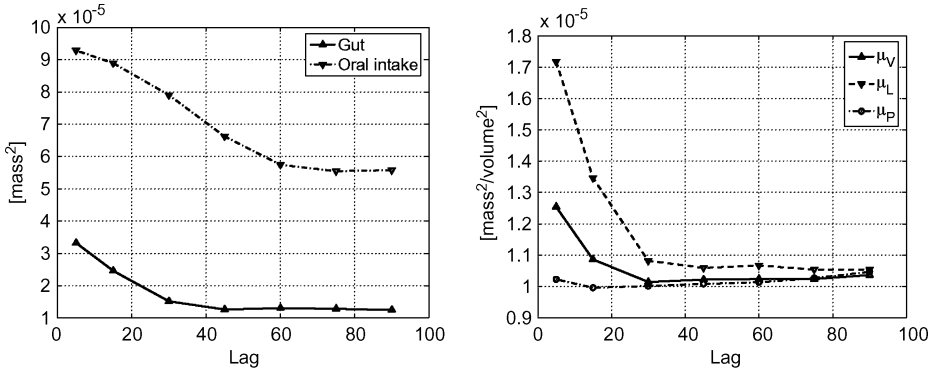

Fig. 2. MSE for the EKF estimates as a function of the number of lags in the EKF. The input is the binge drinker from the set of nine prototypical clinical oral ethanol input trajectories described in Section IV. (a) MSE for the oral input and gut absorption variables; (b) MSE for the three concentrations in the PBPK model.

the estimator to conserve this quantity. Therefore, we define a second criterion, denoted by AREA, by

$$AREA = \left| \int M_{\mathrm{Oral}}(t)\mathrm{d}t - \int \hat{M}_{\mathrm{Oral}}(t)\mathrm{d}t \right| / \int M_{\mathrm{Oral}}(t)\mathrm{d}t \tag{12}$$

which measures how well the estimator determines the total amount of ethanol consumed. The last criterion measures the timing accuracy of the estimated oral input time series. It is important to measure this quantity since a practical approach is to consider the oral consumption time series as periods of drinking alternating with periods of no drinking. Two quantities, $T_{\mathrm{On-Off}}$ and $T_{\mathrm{Off-On}}$, are computed as follows. First, each estimated transition is matched to the true transition closest in time to the estimated transition even if this means that one true transition is matched to two estimated transitions, or that a true transition is left unmatched. Second, the sample means and variances of the difference between true and estimated times are computed, omitting differences greater than 60 min.

A. Statistical Results

A total of 70 sequences, each seven days in duration, were generated from the entire model, i.e., EC, Gut, PBPK, and sensor. Let ω be the quantity of interest. Approximations to the mean and variance of ω were computed by time averaging ω over a seven- day sequence and then the sample mean and variance of ω were computed by averaging over the 70 sequences. The parameter values of the Gut model and the PBPK model are described in Section IV except for the mark level, m_m, which is 0.22 mg/min. The sensor model has one parameter, the noise standard deviation σ, which was 0.05 of the maximum level of the alcohol concentration on the peripheral tissue where the 0.05 value was based on preliminary data for the sensor. The sampling interval T for the sensor is set to 1 min. The sampling interval T_h used in the forward Euler discretization is set to 1 min.

Fig. 2 shows the effect on EKF performance of the number of lags in terms of MSEs for all the states (oral input, mass flow in the Gut model, and the three concentrations in the PBPK model) as a function of the number of lags. The simulator which creates the data and the EKF which analyzes the data share the same parameters. All of the time series except for the oral input are relatively accurately estimated when the size of the lag reaches 50 min while Fig. 2(a) suggests that at least 60 min is required to achieve the best possible performance for the oral input. Based on these and similar results, the value of $L = 60$ min was chosen.

Fig. 3 shows performance, with respect to the three criteria, as a function of sensor noise to signal ratio (NSR) for a range of NSRs around the nominal NSR which is 5%, i.e., the NSR for which the sensor noise standard deviation is 5% of the peak signal value. The range is $(1 - .3)5\%$ to $(1 + .9)5\%$. The first measure of performance is the oral input MSE. The complete three-stage algorithm shows improved performance over the initial stage as the sensor NSR increases (i.e., the right edge of the plot) in Fig. 3(a). With respect to the AREA criterion, as shown in Fig. 3(b), while the Stage 1 algorithm (the EKF) performs rather poorly, the Stage 3 algorithm achieves a satisfactory 10% error. Finally, as shown in Fig. 3(c) regarding timing accuracy, the mean error for both Off to On and On to Off is less than 10 min until the high end of the NSR range (i.e., the right edge of the plot). This is rather good performance considering the amount of low pass filtering that exists between the oral input and the sensor measurement.

B. Results on Prototypical Clinical Oral Ethanol Input Trajectories

As described in Section IV, sensor time series data can be computed from the nine prototypical clinical oral ethanol input trajectories as inputs to the generative model, with the parameter values of Section IV. As a part of this computation, simulated time series data for all of the other time series in the generative model are also computed including the concentrations of ethanol in the portal vein, liver, arteries, veins, and peripheral tissue. Since these concentrations can differ substantially, it is of pharmacokinetic interest and possibly of clinical interest to estimate all of these time series from sensor data.

As indicated in Section II-C, it is challenging to state statistical models for the clinical oral input time series because of their unusual properties. For instance, there are both daily and weekly patterns. Therefore, the success of the estimators on

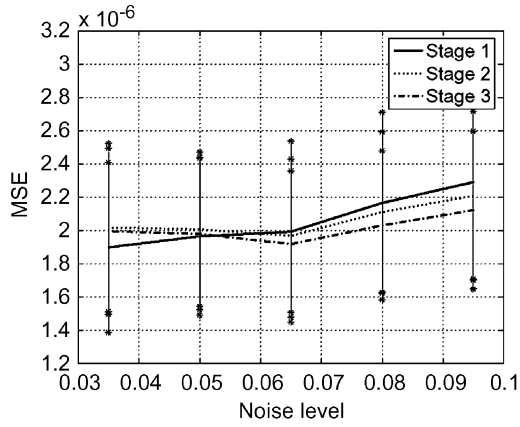

(a)

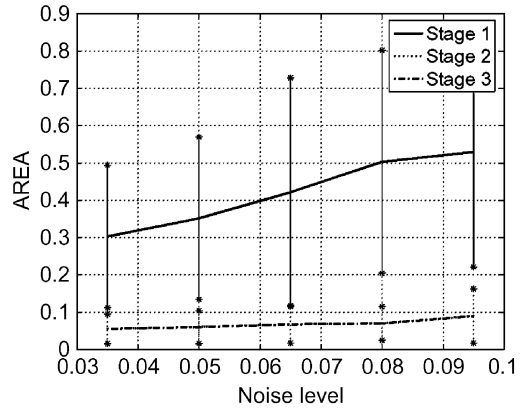

(b)

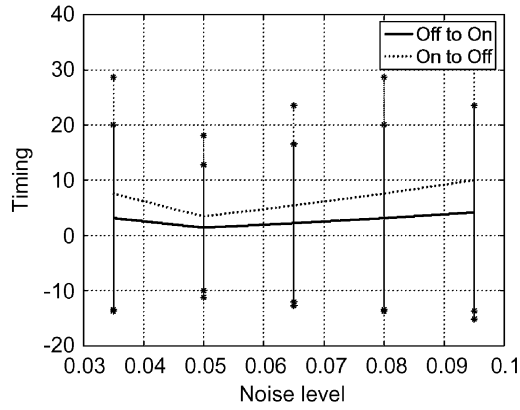

(c)

Fig. 3. MSE (a), *AREA* [(ethanol conservation, (b)], and $T_{\mathrm{On-Off}}$ and $T_{\mathrm{Off-On}}$ [timing of transitions from drinking to no drinking and visa versa, (c)] results as a function of sensor noise to signal ratio (NSR) for Stage 1 and Stage 3 oral input estimates. The error bars indicate ± 1 sample standard deviations. In (b), the Stage 2 result is superimposed on the Stage 3 result.

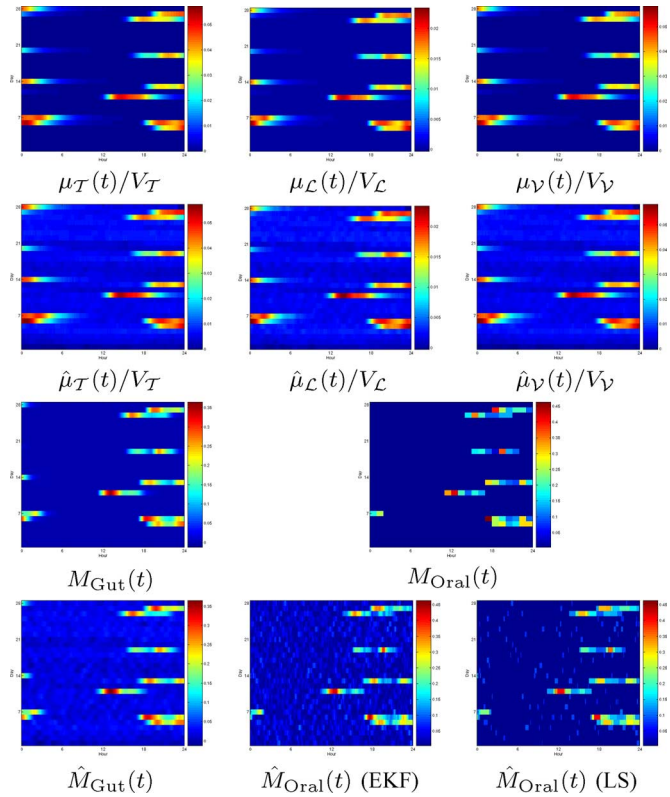

Fig. 4. Results for the binge drinker.

TABLE I
PERFORMANCE FOR THE ENTIRE SET OF PROTOTYPICAL CLINICAL ORAL ETHANOL INPUT TRAJECTORIES WITH THE MATCHED OR THE MISMATCHED ESTIMATORS. ALL PERFORMANCE MEASURES CONCERN THE ORAL INPUT $M_{\mathrm{oral}}(t)$. EACH TRIPLE OF ROWS CONCERNS ON THE ESTIMATES WITH MATCHED PARAMETERS AND SENSOR MODEL, WITH THE MISMATCHED GUT PARAMETER WITH THE DEVIATION OF 30%, AND WITH THE ALTERNATIVE SENSOR MODEL (CCV MODEL), RESPECTIVELY

Case	Stage	MSE ($\times 10^{-6}$mg^2)	AREA (%)	On to Off (min) (Off to On (min))
Matched	EKF	0.23 ± 0.11	0.47 ± 0.32	7.30 ± 10.50 (8.06 ± 11.33)
	DP	0.21 ± 0.09	0.07 ± 0.08	
	LS	0.19 ± 0.09	0.06 ± 0.05	
β with 30% deviation	EKF	0.26 ± 0.13	0.45 ± 0.33	10.19 ± 13.10 (10.41 ± 13.64)
	DP	0.21 ± 0.09	0.09 ± 0.06	
	LS	0.19 ± 0.08	0.07 ± 0.05	
Alternative Sensor model	EKF	0.19 ± 0.09	0.51 ± 0.35	17.22 ± 14.26 (20.20 ± 14.84)
	DP	0.20 ± 0.10	0.03 ± 0.04	
	LS	0.18 ± 0.09	0.04 ± 0.03	

these prototypical clinical oral ethanol input trajectories is potentially of greater importance than the success of the estimator on statistically-generated time series.

Fig. 4 displays the true and estimated time series for one of the prototypical clinical oral ethanol input trajectories, specifically, the binge drinker. Performance in estimating the PBPK variables, $\mu_{\mathcal{T}}(t)/V_{\mathcal{T}}$, $\mu_{\mathcal{L}}(t)/V_{\mathcal{L}}$, and $\mu_{\mathcal{V}}(t)/V_{\mathcal{V}}$, and on the Gut output, $M_{\mathrm{Gut}}(t)$, is quite good. Performance in estimating the oral input, $M_{\mathrm{Oral}}(t)$, is not as good because the oral input is separated from the other variables by the Gut and the Gut is a low pass filter with a low cutoff frequency. Nonetheless, extensive information about the oral input is still determined by the estimator from the sensor measurements. The three performance criteria are tabulated in the first triple of rows in Table I. The MSE performance improves through each stage of the processing. The AREA performance, i.e., ethanol conservation, improves dramatically between the first and second stages and then improves further with the third stage to a final value of 5%. The timing of transitions (third stage only) is accurate to ± 10 min.

C. Results on Stochastic Trajectories Generated From Prototypical Clinical Oral Ethanol Input Trajectories

The prototypical clinical oral ethanol input trajectories are idealizations of the true drinking patterns. In particular, the trajectories are piecewise constant over intervals of an hour (denoted by Δ). In order to more fully demonstrate the performance of our algorithm, we desire more realistic and stochastic examples. It is difficult to construct a statistical model of these time series containing just a few parameters due to the long correlation time (e.g., one week) of the time series. Therefore, we constructed a statistical model for how to perturb the existing prototypical clinical oral ethanol input trajectories. Three types of change are considered. The first is to dither the transitions in the time series by random delays drawn from a pdf that is uniform on $[-\delta/2, \delta/2]$ where δ has units of time. The second is to allow many changes in drinking rate during the interval of drinking by dividing the interval (now with dithered endpoints) into subintervals of duration δ. Whether drinking occurs during a subinterval is determined by a Bernoulli process with success (i.e., does drink) probability of p. The third is to randomize the drinking rate in any subinterval for which drinking occurs. In particular, for each subinterval in which a Bernoulli success occurs, the rate is proportional, with proportionality constant $1/p$, to an i.i.d. random variable drawn from a pdf which is the empirical pdf for that particular prototypical clinical oral ethanol input trajectory. In the other subintervals, the rate is zero. By having only a fraction of p intervals with drinking but scaling the amount of drinking by $1/p$, the expected amount of drink is equal to the amount that occurred in the prototypical clinical oral ethanol input trajectory. However, the variance of the total amount of drink is $Q^2(1-p)/Np$ where Q is the total amount of drink in the prototypical clinical oral ethanol input trajectory and $N = \Delta/\delta$. In order for the standard deviation of the total amount of drink to be small, it is necessary for p to be near 1. In particular, in order to achieve a standard deviation that is 20% of the mean, p was chosen to be 0.75 since the ratio of standard deviation to mean is $\sqrt{(1-p)/(Np)}$.

Oral inputs were simulated for a variety of values for δ in the range of 6 to 30 min (recall that the prototypical clinical oral ethanol input trajectories were piecewise constant over 1 h intervals). These simulations were then used as input to the Gut, PBPK, and sensor systems in order to generate the corresponding sensor time series. These time series were processed as described previously with the exception that in Step 3, the window for the least squares calculation is duration δ, not Δ. Performance statistics were computed as described previously in Section VI-A and are graphed in Fig. 5. Comparing Figs. 3 and 5, performance is at least as good on the stochastic trajectories generated from the prototypical clinical oral ethanol input trajectories as it is (same 5% NSR level) on the prototypical clinical oral ethanol input trajectories themselves.

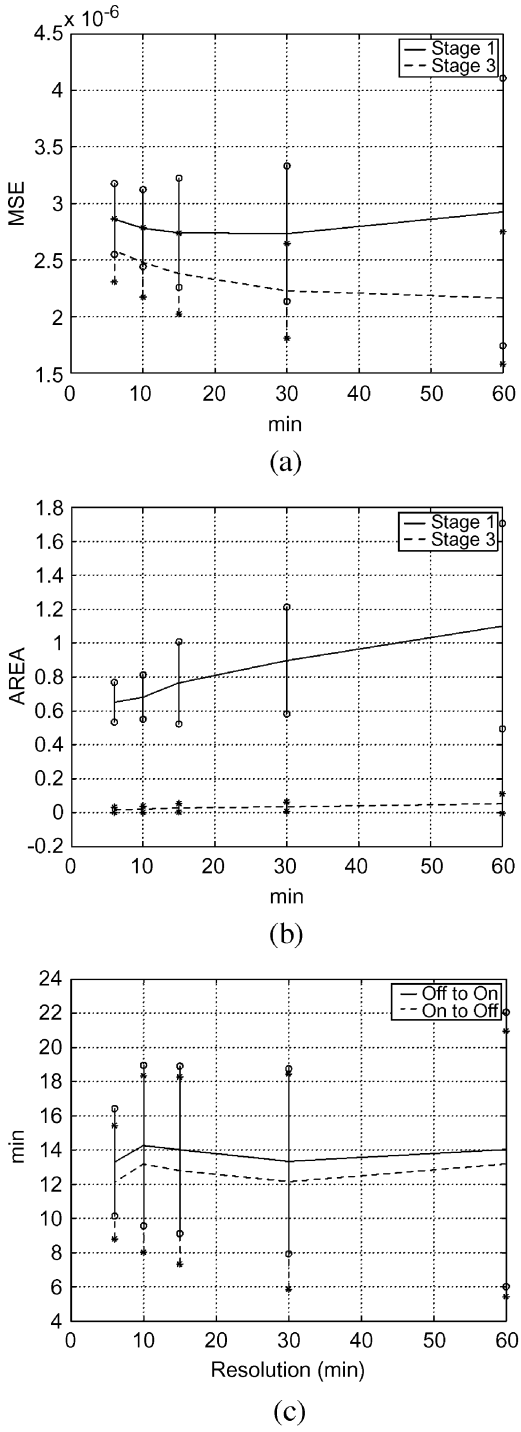

Fig. 5. Results based on a stochastic version of the lunch and dinner drinker prtotypical clinical oral ethanol input trajectory plotted as a function of the time δ at an NSR of 5%. MSE (a), *AREA* [ethanol conservation, (b)], and $T_{\mathrm{On-Off}}$ and $T_{\mathrm{Off-On}}$ [iming of transitions from drinking to non drinking and visa versa, (c)] esults as a function of sensor NSR for Stage 1 and Stage 3 oral input estimates. The error bars indicate $\pm$ sample standard deviasons.

D. Results on the Cases With Mismatched Model and Parameters

Since the parameters in the PBPK model and the mark levels in the EC model are obtained from system identification procedures, in this section calculations demonstrating robustness to parameter variation focused on variation in the one parameter β of the Gut model and alteration in the form of the sensor model are presented. The variation in β is 30% of the nominal value and the alteration in the form of the sensor model is to use a CCV (constant coefficient of variation, see Section II-D) model with the same noise level used in the nominal model. In

all instances, time series are generated using the altered β or the CCV sensor model and then processed using the nominal β or the nominal sensor model. Table I shows the results achieved for each case: matched, β variation, and CCV sensor model. Using the MSE and AREA criteria, the estimation is robust since performance in the two mismatched cases is essentially the same as the matched case. Using the timing criteria (On to Off and Off to On) performance is reduced but the uncertainty is still substantially smaller than the discretization that satisfactorily described the clinical situation, as reflected in the prototypical clinical oral ethanol input trajectories.

VII. Discussion

In this paper, a three-stage algorithm is described for estimating liver, blood, and peripheral tissue ethanol concentrations and ethanol ingestion from sensor time series measurements of interstitial fluid ethanol concentration. The computational complexity is low, in part because it is possible to exploit multiple sampling rates in the EKF. The algorithm exploits the fact that only batch processing is needed in order to be adaptive to the data. With regard to the estimated oral ethanol input, the goal is really to tell a story, i.e., that drinking started and stopped at certain times with a certain total amount consumed. Thus, we consider a variety of performance measures that focus on such stories in addition to MSE. We believe that the signal processing system described here is sufficient to meet the goals of the alcohol research community, and may be the best that can be achieved because of the extensive nonlinear low pass filtering the occurs between the oral input and the sensor data. With this system, we are able to provide clinically-relevant levels of performance both in Monte Carlo simulation and with the nine prototypical clinical oral ethanol input trajectories based on clinical practice. Sensor experimental data is not yet available because this project, though funded by NIH, is being run using the DARPA co-development model and the sensor is only now about to enter in vivo testing in animal models. Development of the sensor is costly, but the "planning" analysis carried out in this paper justifies the expectation that the sensor and signal processing system will be able to achieve the sponsor's objectives.

During the next two years, we expect to replicate this work with experimental data as data from sensors implanted in rats become available. The PBPK models of alcohol absorption, distribution and elimination easily scale across species and alcohol research in rodents affords a complete record of the time course of ingested alcohol consumption for each animal. All the signal processing described here will be directly applicable to these experiments.

Appendix I
Equations for the PBPK Model

The PBPK model is composed of three nonlinear ordinary differential equations for the state variables (13)–(15)

$$\frac{\mathrm{d}\mu_{\mathcal{L}}}{\mathrm{d}t}(t) = M_{\mathrm{HA},\mathcal{L}}(t) + M_{\mathrm{PV},\mathcal{L}}(t) - M_{\mathcal{L},\mathrm{HV}}(t) - M_{\mathrm{Metab}}(t) \tag{13}$$

$$\frac{\mathrm{d}\mu_{\mathcal{T}}}{\mathrm{d}t}(t) = M_{\mathrm{P},\mathcal{T}}(t) - M_{\mathcal{T},\mathrm{P}}(t) \tag{14}$$

$$\frac{\mathrm{d}\mu_{\mathcal{V}}}{\mathrm{d}t}(t) = -M_{\mathrm{HA},\mathcal{L}}(t) - M_{\mathrm{PV},\mathcal{L}}(t) + M_{\mathcal{L},\mathrm{HV}}(t) + M_{\mathcal{T},\mathrm{P}}(t) - M_{\mathrm{P},\mathcal{T}}(t) + M_{\mathrm{Infuse}}(t) + M_{\mathrm{Gut}}(t) \tag{15}$$

where the subscriptions are PV for portal vein, HA for hepatic artery, and HV for hepatic vein; the eight mass flux equations needed to evaluate (13)–(15), which are the two external inputs $M_{\mathrm{Gut}}(t)$ and $M_{\mathrm{Infuse}}(t)$ and the six internal variables $M_{\mathrm{Metab}}(t)$, $M_{\mathrm{P},\mathcal{T}}(t)$, $M_{\mathcal{T},\mathrm{P}}(t)$, $M_{\mathrm{HA},\mathcal{L}}(t)$, $M_{\mathrm{PV},\mathcal{L}}(t)$, and $M_{\mathcal{L},\mathrm{HV}}(t)$ [(16), (17), (18), (19), (20), and 21, respectively]

$$M_{\mathrm{Metab}}(t) = V_{\mathcal{L}} V_{\max} \frac{\mu_{\mathcal{L}}(t)/V_{\mathcal{L}}}{K_m + \mu_{\mathcal{L}}(t)/V_{\mathcal{L}}} \tag{16}$$

$$M_{\mathrm{P},\mathcal{T}}(t) = k_{\mathrm{P},\mathcal{T}} R_{\mathrm{A}} (1 - F_{\mathrm{L}}) r \left(\frac{\mu_{\mathcal{V}}(t)}{V_{\mathcal{V}}} - \frac{\mu_{\mathcal{T}}(t)}{V_{\mathcal{T}}} \right) \tag{17}$$

$$M_{\mathcal{T},\mathrm{P}}(t) = k_{\mathcal{T},\mathrm{P}} R_{\mathrm{A}} (1 - F_{\mathrm{L}}) r \left(\frac{\mu_{\mathcal{T}}(t)}{V_{\mathcal{T}}} - \frac{\mu_{\mathcal{V}}(t)}{V_{\mathcal{V}}} \right) \tag{18}$$

$$M_{\mathrm{HA},\mathcal{L}}(t) = k_{\mathrm{HA},\mathcal{L}} R_{\mathrm{A}} F_{\mathrm{L}} (1 - F_{\mathrm{PV}}) \times r \left(\frac{\mu_{\mathcal{V}}(t)}{V_{\mathcal{V}}} - \frac{\mu_{\mathcal{L}}(t)}{V_{\mathcal{L}}} \right) \tag{19}$$

$$M_{\mathrm{PV},\mathcal{L}}(t) = k_{\mathrm{PV},\mathcal{L}} R_{\mathrm{A}} F_{\mathrm{L}} F_{\mathrm{PV}} \times r \left(\frac{\mu_{\mathcal{V}}(t)}{V_{\mathcal{V}}} + \frac{M_{\mathrm{Gut}}(t)}{R_{\mathrm{A}} F_{\mathrm{L}} F_{\mathrm{PV}}} - \frac{\mu_{\mathcal{L}}(t)}{V_{\mathcal{L}}} \right) \tag{20}$$

$$M_{\mathcal{L},\mathrm{HV}}(t) = k_{\mathcal{L},\mathrm{HV}} R_{\mathrm{A}} F_{\mathrm{L}} r \left(\frac{\mu_{\mathcal{L}}(t)}{V_{\mathcal{L}}} - C_{\mathrm{HV}}(t) \right) \tag{21}$$

$M^{(2)}_{\mathrm{PV}}(t)$ and $M_{\mathrm{HA}}(t)$ [(22) and (23), respectively]

$$M^{(2)}_{\mathrm{PV}}(t) = \frac{\mu_{\mathcal{V}}(t)}{V_{\mathcal{V}}} R_{\mathrm{A}} F_{\mathrm{L}} F_{\mathrm{PV}} + M_{\mathrm{Gut}}(t) \tag{22}$$

$$M_{\mathrm{HA}}(t) = R_{\mathrm{A}} F_{\mathrm{L}} (1 - F_{\mathrm{PV}}) \frac{\mu_{\mathcal{V}}(t)}{V_{\mathcal{V}}} \tag{23}$$

and

$$C_{\mathrm{HV}}(t) = \begin{cases} 1/1 + k_{\mathcal{L},\mathrm{HV}}(\alpha(t) + k_{\mathcal{L},\mathrm{HV}}\gamma(t)), & \alpha(t) < \gamma(t) \\ \alpha(t), & \alpha(t) > \gamma(t) \end{cases},$$

where $\gamma(t) = \mu_{\mathcal{L}}(t)/V_{\mathcal{L}}$ and

$$\alpha(t) = \frac{1}{R_{\mathrm{A}} F_{\mathrm{L}}} \left(M_{\mathrm{HA}}(t) - M_{\mathrm{HA},\mathcal{L}}(t) + M^{(2)}_{\mathrm{PV}}(t) - M_{\mathrm{PV},\mathcal{L}}(t) \right).$$

The following constants are required: the volumes of the three compartments, denoted by $V_{\mathcal{V}}$, $V_{\mathcal{L}}$, and $V_{\mathcal{T}}$; the Michaelis-Menten constants, denoted by $V_{\max}$ and K_m; the cardiac output, denoted by R_{A}; the fraction of cardiac output that is delivered to the liver and the fraction of the total liver supply that is delivered by the portal vein, denoted by F_{L} and F_{PV}, respectively, and the fraction of ethanol in a vessel or compartment that is transported to a connected vessel or compartment, denoted by $k_{\mathrm{P},\mathcal{T}}$, $k_{\mathcal{T},\mathrm{P}}$, $k_{\mathrm{HA},\mathcal{L}}$, $k_{\mathrm{PV},\mathcal{L}}$, and $k_{\mathcal{L},\mathrm{HV}}$. The right hand sides of (13)–(15) define the functions $f_{\mathcal{L}}(\cdot)$, $f_{\mathcal{T}}(\cdot)$, and $f_{\mathcal{V}}(\cdot)$, respectively.

Appendix II
Gaussian Equivalent Model for a Singly-Stochastic Version of the EC Model

For $t \in \mathbb{R}$ let $x(t) \in \{0, 1\}$ be the state of a two-state continuous-time discrete-state Markov chain with constant rate parameters $\lambda_{1,2}$ and $\lambda_{2,1}$. Let t_k for $k \in \mathcal{Z}$ be the transition times.

Let $m[k]$ be the mark chosen at the kth transition. The sequence of marks are independent random variables. Since there are only two states, the pmf on the mark, which depends on the old and new states at the transition, actually depends only on the new state which is $x(t_k)$. Define $\bar{m}_i = E[m[k]|x(t_k) = i]$ and $\sigma_i^2 = \mathrm{Var}[m[k]|x(t_k) = i]$. With this notation, the output of the EC model is $M_{\mathrm{Oral}}(t) = \sum_{k=-\infty}^{+\infty} m[k][u(t-t_k)-u(t-t_{k+1})]$. For the Markov chain $x(t)$, the infinitesimal rate matrix, denoted by Λ, is [7, Chap. 4, Sec. 8, pp. 150–152] $\Lambda_{1,1} = -\lambda_{1,2}$, $\Lambda_{1,2} = \lambda_{1,2}$, $\Lambda_{2,1} = \lambda_{2,1}$, and $\Lambda_{2,2} = -\lambda_{2,1}$, and if $P_{i,j}(t)$ is defined by $P_{i,j}(t) \doteq \Pr(x(t+s) = j|x(s) = i)$ and $P(t)$ is the matrix with elements $P_{i,j}(t)$ then [7, Chap. 4, Sec. 8, pp. 150–152], for $t \geq 0$ (see the equation shown at the bottom of the page). Define $\pi_i(t) \doteq \Pr(x(t) = i)$. The expected value of the output is

$$\bar{M}_{\mathrm{Oral}}(t) \doteq E\left[M_{\mathrm{Oral}}(t)\right] = \sum_{i\in\{0,1\}} \bar{m}_i \pi_i(t). \qquad (24)$$

The Markov chain is assumed to start in the steady state, which is $\pi(\infty) = (1/(\lambda_{1,2} + \lambda_{2,1}))[\lambda_{2,1}, \lambda_{1,2}]$ and in the steady state (24) simplifies to $\bar{M}_{\mathrm{Oral}}(\infty) = \bar{m}_1\pi_1(\infty) + \bar{m}_2\pi_2(\infty)$. The autocorrelation function of the output is $R_{M_{\mathrm{Oral}}}(t_1, t_2) \doteq E[M_{\mathrm{Oral}}(t_1)M_{\mathrm{Oral}}(t_2)] = E[m[k_1]m[k_2]]$ where k_1 is such that $t_{k_1} \leq t_1 < t_{k_1+1}$ and k_2 is such that $t_{k_2} \leq t_2 < t_{k_2+1}$. By the total probability theorem

$$R_{M_{\mathrm{Oral}}}(t_1,t_2) = \sum_{j_1=1}^{2}\sum_{j_2=1}^{2} E\left[m[k_1]m[k_2]|x(t_1)=j_1, x(t_2)=j_2\right] \times \Pr\left(x(t_1)=j_1, x(t_2)=j_2\right).$$

When $j_1 \neq j_2$ it follows that $m[k_1]$ and $m[k_2]$ are independent random variables. However, when $j_1 = j_2$ it is possible that $k_1 = k_2$ ($m[k_1]$ and $m[k_2]$ are the same random variable, described below as "no transition") or that $k_1 \neq k_2$ ($m[k_1]$ and $m[k_2]$ are independent random variables, described below as "transition"). Assume that $t_1 \geq t_2$, condition on the "transition" and "no transition" events, use the fact that the probability $\Pr(x(t_1) = 1, x(t_2) = 1$, no transition) is the probability that an exponentially distributed random variable (parameter $\lambda_{1,2}$) is larger than $t_1 - t_2$, write $t_1 = t$ and $t_2 = t - \tau$, and assume that the $x(\cdot)$ process was started in the steady state to get that

$$R_{M_{\mathrm{Oral}}}(\tau) = \left[\bar{M}_{\mathrm{Oral}}(\infty)\right]^2 + \sigma_1^2 e^{-\lambda_{1,2}\tau} + \sigma_2^2 e^{-\lambda_{2,1}\tau} + \pi_1(\infty)\pi_2(\infty)(\bar{m}_1 - \bar{m}_2)^2 e^{-\tau(\lambda_{1,2}+\lambda_{2,1})}. \qquad (25)$$

Since $M_{\mathrm{Oral}}(t)$ is real-valued, it follows that $R_{M_{\mathrm{Oral}}}(-\tau) = R_{M_{\mathrm{Oral}}}(\tau)$ and, therefore, (25), which is restricted to $\tau \geq 0$, can be generalized to arbitrary $\tau \in \mathbb{R}$ by replacing τ by $|\tau|$. The autocovariance function, $C_{M_{\mathrm{Oral}}}(\tau)$, is $C_{M_{\mathrm{Oral}}}(\tau) = R_{M_{\mathrm{Oral}}}(\tau) - [\bar{M}_{\mathrm{Oral}}(\infty)]^2$ which has Fourier transform

$$S_{M_{\mathrm{Oral}}}(f) = \frac{2\sigma_1^2\lambda_{1,2}}{(\lambda_{1,2}+j2\pi f)(\lambda_{1,2}-j2\pi f)} + \frac{2\sigma_2^2\lambda_{2,1}}{(\lambda_{2,1}+j2\pi f)(\lambda_{2,1}-j2\pi f)} + \frac{2\pi_1(\infty)\pi_2(\infty)(\bar{m}_1-\bar{m}_2)^2(\lambda_{1,2}+\lambda_{2,1})}{(\lambda_{1,2}+\lambda_{2,1}+j2\pi f)(\lambda_{1,2}+\lambda_{2,1}-j2\pi f)}$$

which is rational. Therefore, it can be realized as a finite-dimensional linear system driven by a zero-mean white noise with power spectral density 1 which in turn can be realized as a finite-dimensional continuous-time state-space system [20, Chap. 2, Sec. 2.9, pp. 33–34] and one such realization is described in the body of the paper.

REFERENCES

[1] M. A. Schuckit, T. L. Smith, G. P. Danko, J. Kramer, J. Godinez, K. K. Bucholz, J. I. Nurnberger, Jr., and V. Hesselbrock, "Prospective evaluation of the four DSM-IV criteria for alcohol abuse in a large population," *Amer. J. Psych.*, vol. 162, no. 2, pp. 350–360, Feb. 2005.

[2] H. D. Paykin, "A. Alcohol dependence and abuse diagnoses: Concurrent validity in a nationally respresentative sample," *Alcoholism: Clin. Exp. Res.*, vol. 23, no. 1, pp. 144–150, Jan. 1999.

[3] B. D. O. Anderson and J. B. Moore, *Optimal Filtering*. Englewood Cliffs, NJ: Prentice-Hall, 1979.

[4] L. Stryer, *Biochemistry*, 4th ed. New York: Freeman, 1999.

[5] J.-J. Han, M. H. Plawecki, P. C. Doerschuk, V. A. Ramchandani, and S. O'Connor, "Ordinary differential equation models for ethanol pharmacokinetic based on anatomy and physiology," presented at the IEEE EMBS, Sep. 2006.

[6] M. H. Plawecki, "A physiologically-based pharmacokinetic (PBPK) model for ethanol: Mathematical foundations, parameter identification, and other applications," Ph.D. dissertation, Weldon School Biomed. Eng., Purdue Univ., West Lafayette, IN, May 2005.

[7] S. Karlin and H. M. Taylor, *A First Course in Stochastic Processes*, 2nd ed. San Diego, CA: Academic, 1975.

[8] S. M. Ross, *Stochastic Processes*, 2nd ed. New York: Wiley, 1996.

[9] Y. Bar-Shalom and X. R. Li, *Estimation and Tracking: Principles, Techniques and Software*. Norwell, MA: Artech House, 1993.

[10] S. Haykin, *Kalman Filtering and Neural Networks*. New York: Wiley, 2001.

[11] E. Mazor, J. Dayan, A. Averbuch, and Y. Bar-Shalom, "Interacting multiple model methods in target tracking: A survey," *IEEE Trans. Aerosp. Electron. Syst.*, vol. 34, no. 1, pp. 103–123, Jan. 1998.

[12] R. Togneri and L. Deng, "Joint state and parameter estimation for a target-directed nonlinear dynamic system model," *IEEE Trans. Signal Process.*, vol. 51, no. 12, pp. 1361–1370, Dec. 2003.

[13] A. D. Poularikas and S. Seely, *Signals And Systems*, 2nd ed. Boston, MA: PWS-KENT, 1990.

[14] D. Clements and B. D. O. Anderson, "A nonlinear fixed-lag smoother for finite-state Markov processes," *IEEE Trans. Info. Theory*, vol. 21, no. 4, pp. 446–452, Jul. 1975.

[15] J.-J. Han, "Statistical signal processing and pattern recognition for an implanted ethanol biosensor," Ph.D. dissertation, School Elect. Comput. Eng., Purdue Univ., West Lafayette, IN, Aug. 2006.

[16] S. O'Connor, V. A. Ramchandani, and T.-K. Li, "PBPK modeling as a basis for achieving a steady BrAC of 60 ± 5 mg% within ten minutes," *Alcohol Clin. Exp. Res.*, vol. 24, pp. 426–427, 2000.

$$P(t) = \exp(\Lambda t) = \frac{1}{\lambda_{1,2}+\lambda_{2,1}} \begin{bmatrix} \lambda_{2,1} + \lambda_{1,2}e^{-t(\lambda_{1,2}+\lambda_{2,1})} & -\lambda_{1,2}\left(e^{-t(\lambda_{1,2}+\lambda_{2,1})} - 1\right) \\ -\lambda_{2,1}\left(e^{-t(\lambda_{1,2}+\lambda_{2,1})} - 1\right) & \lambda_{1,2} + \lambda_{2,1}e^{-t(\lambda_{1,2}+\lambda_{2,1})} \end{bmatrix}$$

[17] M. H. Plawecki, R. A. DeCarlo, V. A. Ramchandani, and S. O'Connor, "Estimation of ethanol infusion profile to produce specified BrAC time course using physiologically-based pharmacokinetic (PBPK) models," presented at the IEEE EMBS, Sep. 2004.
[18] D. P. Bertsekas and J. Tsitsiklis, *Neuro-Dynamic Programming*. Belmont, MA: Athena Scientific, 1996.
[19] L. R. Rabiner, "A tutorial on hidden Markov models and selected applications in speech recognition," *Proc. IEEE*, vol. 77, no. 2, pp. 257–286, Feb. 1989.
[20] B. Porat, *Digital Processing of Random Signals: Theory and Methods*. Englewood Cliffs, NJ: Prentice-Hall, 1994.

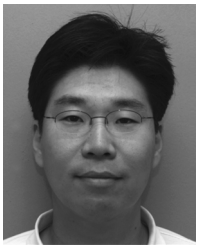

Jae-Joon Han (M'07) received the B.S. degree in electronic engineering from Yonsei University, Korea, in 1997, the M.S. degree in electrical and computer engineering from the University of Southern California, Los Angeles, in 2001, and the Ph.D. degree in electrical and computer engineering from Purdue University, West Lafayette, IN, in August 2006.

From 2001 to 2006, he was a Teaching Assistant and then a Research Assistant in the School of Electrical and Computer Engineering, Purdue University. Since receiving the Ph.D. degree, he has continued at Purdue as a Postdoctoral Fellow pursuing research in biomedical modeling and stochastic inference.

Peter C. Doerschuk (SM'03) received the B.S., M.S., and Ph.D. degrees in electrical engineering from the Massachusetts Institute of Technology (MIT), Cambrige, and the M.D. degree from Harvard Medical School, Cambridge.

After postgraduate training at Brigham and Womens' Hospital, Boston, he held a postdoctoral appointment at the Laboratory for Information and Decision Systems, MIT, from January 1988 to August 1990. After 16 years on the faculty of Electrical and Computer Engineering, Purdue University, West Lafayette, IN, he joined the faculty of Biomedical Engineering and Electrical and Computer Engineering at Cornell University, Ithaca, NY, in July 2006.

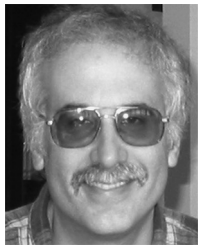

Saul B. Gelfand received the Ph.D. degree in electrical engineering and computer science from the Massachusetts Institute of Technology (MIT), Cambrige, in 1987.

Previously, he was with Scientific Systems, Inc., Cambridge, and Bolt Beranek and Newman, Inc., Cambridge, where he worked on multitarget detection and tracking problems in sonar signal processing. Since 1987, he has been with Electrical and Computer Engineering, Purdue University, West Lafayette, IN, where he is a Professor. His major contributions lie in the formulation and analysis of recursive algorithms for detection, estimation, filtering, and optimization of stochastic systems. His research is supported by the National Science Foundation, the National Institutes of Health, the Army Research Office, Thomson Multimedia, and Lucent Technologies.

Prof. Gelfand has previously served as an Associate Editor for Equalization for the IEEE TRANSACTIONS ON COMMUNICATIONS and Chair of the Communications Theory Symposium at the *2000 IEEE International Conference on Communication*.

Sean J. O'Connor is a faculty member in psychiatry at the Indiana University School of Medicine and Biomedical Engineering, Purdue University, West Lafayette. He divides his time between research, clinical care, and teaching. His research focuses on the genetic determinants of the human brain's adaptive response to alcohol. He directs three laboratories where subjective perceptions, neuropsychologic tests, eye movements, and EEG are used to characterize the ways people who are more vulnerable to future alcoholism respond differently to alcohol when compared to controls.